CHARACTERIZATION OF LAND DEGRADATION AT THE ÑACUÑÁN BIOSPHERE RESERVE IN ARGENTINA WITH AVIRIS DATA

Alfredo Huete,[1] Tomoaki Miura,[1] Xiang Gao,[1] Carlos Borghi,[2] and Ricardo Ojeda[2]
[1]Department of Soil, Water and Environmental Science, University of Arizona, Tucson, Arizona 85721, USA
ahuete@ag.arizona.edu; tomoaki@ag.arizona.edu; xgao@ag.arizona.edu
[2]Instituto Argentino de Investigaciónes de las Zonas Aridas (IADIZA), Mendoza, Argentina

I. INTRODUCTION

Land degradation impacts on several critical environmental issues such as food security, diminishing quality and quantity of fresh water resources, preservation of natural resources, loss of biodiversity, and global climate change. Land degradation is responsible for soil erosion and can eventually lead to desertification. The International Convention to Combat Desertification (CCD) defines desertification as "land degradation in arid, semi-arid, and dry sub-humid areas resulting from various factors, including climate variations and human activity". The resulting loss of soil cover, the loss of genetic diversity, the physical and chemical degradation of soils, and sedimentation of river basins and dams creates major environmental constraints for sustainable development.

General information and data regarding the degree and extent of land degradation are lacking and effective monitoring and detection programs are hampered by the lack of a comprehensive set of guidelines for survey, assessment, and monitoring of land degradation, including early warning indicators. Remote sensing offers a quantifiable and replicable technique to assess desertification under a unified methodology at regional and global scales. To manage or reverse land degradation, one needs early warning signals, given the high costs for remediation. There are many indicators of land degradation and desertification, many of which lend themselves to remote sensing- based monitoring. These include (1) loss of vegetative cover; (2) changes in vegetation composition; (3) landscape instability due to wind and water erosion; (4) soil salinization; (5) soil structure deterioration; (6) less soil moisture; (7) increases in albedo; and (8) higher land surface temperatures.

Aguiar et al. (1988) produced maps of desertification in Patagonia with NOAA-AVHRR and Landsat MSS. Their methodology included recording data on degradation of vegetative cover and of soil water erosion, wind erosion, soil crusting and compaction, and salinization/alkalinization. Pickup and Nelson (1984) showed that changes in the variance of pixel subareas in Australia could be the most sensitive indicator of landscape instability, with an increase in variance indicating erosion and a decrease in variance indicating the possibility of deposition. In a study on the Jornada Experimental Range in New Mexico, an increase in the spatial and temporal heterogeneity of water, nutrients, and other soil resources has favored the invasion of desert shrubs (Schlesinger et al., 1990). Archer et al, (1995) have coupled shrub invasion mechanisms with climate and land use activities. Indicators of soil erosion and land degradation were the loss of vegetative cover and spatial variation of soil spectral properties owing to the loss of topsoil and exposure of subsoil layers. As erosion proceeds, more of the parent material mineralogies and spectral properties become evident while the optical properties of the organic rich upper layers become less pronounced. The undisturbed, well-developed soil and the underlying parent material represent the two endpoints from which the various degrees of soil erosion and land degradation can be assessed. These characteristics can be monitored with satellite imagery, using spectral indices and mixture models (Tucker and Nicholson, 1999).

Hyperspectral remote sensing has improved the feasibility of unambiguously identifying numerous soil and vegetation absorption features, related to mineralogy, liquid water, chlorophyll, cellulose, and lignin contents (Smith et al., 1990; Gao and Goetz, 1994; Asner and Green, 2002). This is potentially useful in the analysis of land degradation in semiarid regions which often entail simultaneous changes in both soil and vegetation biophysical and optical properties. In this study we attempt to fully characterize a set of natural and altered land cover sites in order

to determine the potential of hyperspectral imagery for characterization of land degradation. Here, we specifically report on the use of spectral mixture analysis and multi-component fraction extracts for assessments of land health.

2. STUDY SITES AND METHODS

The Ñacuñán Biosphere Reserve comprises and area of 12,271 ha at a mean altitude of 540 m and is located in a warm semi-desert shrub land ecosystem in the province of Mendoza (34°02'S; 67°54'W). With an average annual temperature of 15.8 C and 200 mm annual precipitation, the site is characterized by open forests of mesquite (*Prosopis spp*.) and creosote bush (*Larrea divaricata and L. cuneifolia*), locally known as algarrobal and jarillal communities, respectively (Ojeda et al., 1998). These open forest communities were totally cut down between the years 1907 and 1937 and are now protected under a restoration and protection plan. The algarrobal community of mixed mesquite-creosote bush is the main cover type inside the reserve followed by the jarillal (creosote bush) community. The dark green leaves of the creosote bush render this community very dark in appearance in satellite imagery relative to the algarrobal vegetated areas (Fig. 1). There are two additional vegetation formations resulting from previous and current phases of land degradation, including a 'medanal' community consisting of both mesquite and creosote bush species and characterized by sand dune formations and a 'peladal' community which is severely degraded, has stunted creosote bush, and appears very bright (Fig. 1). These degraded vegetation communities are present inside the reserve but are much more prominent outside the reserve, particularly to the north (Fig. 1a).

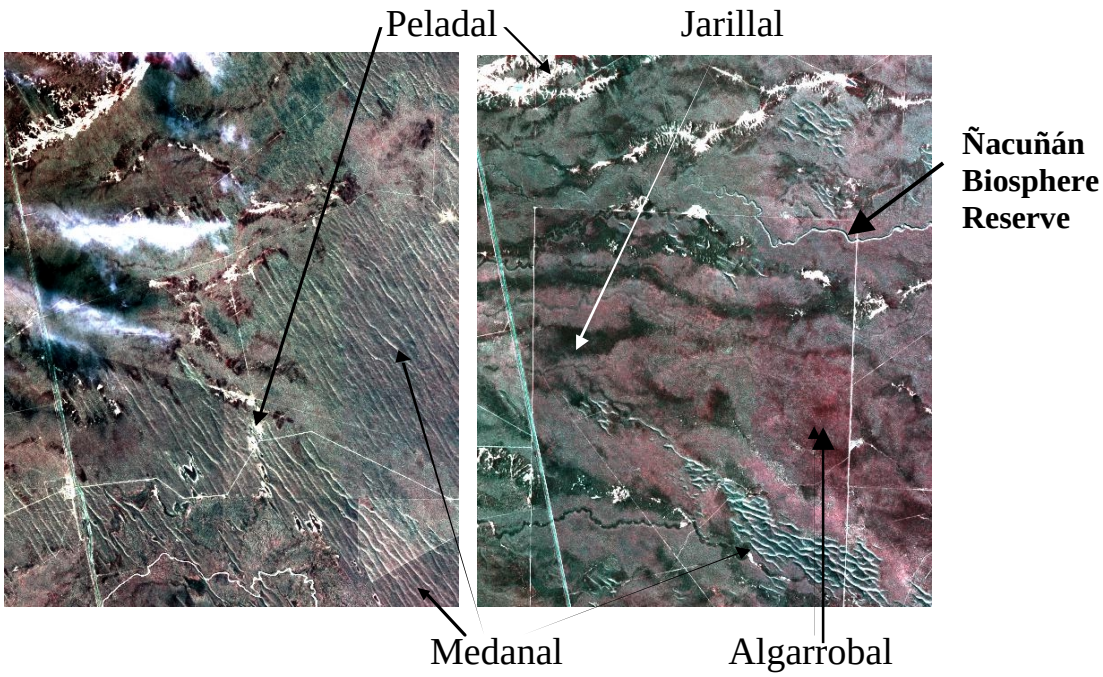

Figure 1. Ikonos image depicting the vegetation communities at the Ñacuñán Biosphere Reserve, Argentina (right) and the extensive degraded areas found north of the Reserve (left).

Field optical and biophysical measurements were conducted from January 28 through February 6, 2001. An ASD FieldSpec radiometer with a spectral range from 370 nm to 1050 nm, and GPS unit were mounted on a yoke device 2 m above the surface and used over 100-m transects for canopy optical characterization. The 100-m transect measurements were only made through the medanal and peladal canopies as the vegetation was too tall for transect measurements in the algarrobal and jarillal communities. In addition, we conducted 50-m transects through two bare soil playas, denuded of vegetation. All ASD spectra were collected between 10am and noon and converted to reflectance values with the use of a standard reference, Spectralon panel. We also made simultaneous measurements of leaf area index (LAI) and fractional component covers (green vegetation (GV), non-photosynthetic vegetation (NPV), litter and soil) along the 100 m transects using the line intercept method with a spacing of 20 cm, yielding 500 cover points per transect.

Low level Airborne Visible/ Infrared Imaging Spectrometer (AVIRIS) flights were made at the Ñacuñan Reserve on February 15, 2001. The AVIRIS imaging spectrometer operates in the 400 to 2450 nm region collecting 224 spectral bands with a nominal 10 nm spectral response function. AVIRIS flew at an altitude of 4 km yielding 4 m pixels. The hyperspectral imagery was corrected for atmosphere and converted to surface reflectances with the aid of an atmosphere correction program, ATREM, constrained with field ASD radiometric measurements. With the aid of GPS data and Ikonos images, we co-registered the averaged ASD field spectra over the denuded playas and peladal areas to serve as the calibration ground control points.

We performed a basic, linear spectral mixture analyses to decompose the AVIRIS data into its fractional components, including a soil component, a non-photosynthetic vegetation (NPV) signal (wood/litter), and a green vegetation (GV) sensitive measure. The basis of the mixture model is that the measured spectral response of a pixel is equal to the weighted sum of multiple reflecting surface features,

$$d_{ik} = \sum_{j=1}^{n} r_{ij}\, c_{jk} + e \qquad (1)$$

where d_{ik} is the measured spectral response of the spectral mixture k in waveband i, n is the number of independent reflecting components in the mixture, r_{ij} is the response of component j in waveband i, c_{jk} is the relative contribution of component j in spectral mixture k, and e is the residual error. In matrix notation, Eq. (1) is expressed as

$$[D] = [R]\ [C] + [e] \qquad (2)$$

where [D] is the spectral data matrix, [R] is the response matrix of the independent reflecting materials or 'endmembers', [C] is the fractional component contributions or 'loadings' matrix, and [e] are the residual errors. The dimensionality, n, represents the number of unique reflecting materials in the mixture data set and is determined with the aid of principal components analysis (PCA), which decomposes the spectral data matrix [D] into an abstract feature matrix $[R]_A$ and an eigenvector matrix $[C]_A$ such that $[D] = [R]_A\ [C]_A$. The abstract-based principal components analysis results were then converted (rotated) into physical-based results through the use of 'endmembers'. We used pure pixel endmembers for the green vegetation and soil endmembers, field-based spectra for the NPV endmember, and a shade endmember was created using a signature of zero reflectances.

3. RESULTS

The averaged spectral signatures (n~100) from the AVIRIS derived reflectances across normal and degraded vegetation communities are depicted in Fig. 2. Most of the transect spectra contain very weak vegetation signals and resemble soil spectra. The two peladal sites consisted of sparse creosote bush with different soil backgrounds, one being darker and more clayey with large dry, cracks on the surface. The moderately degraded medanal site had lower reflectances with a weak, red absorption feature in its signature (Fig. 2). This was nearly equivalent to the spectral signatures of the algarrobal sites. The jarillal vegetation community had the lowest spectral reflectance signature. In the shortwave-infrared (SWIR) region, all the vegetation communities, with the exception of the peladal sites, showed lignin absorption features, allowing for spectral separation of soil from NPV and GV (Asner and Lobell, 2000).

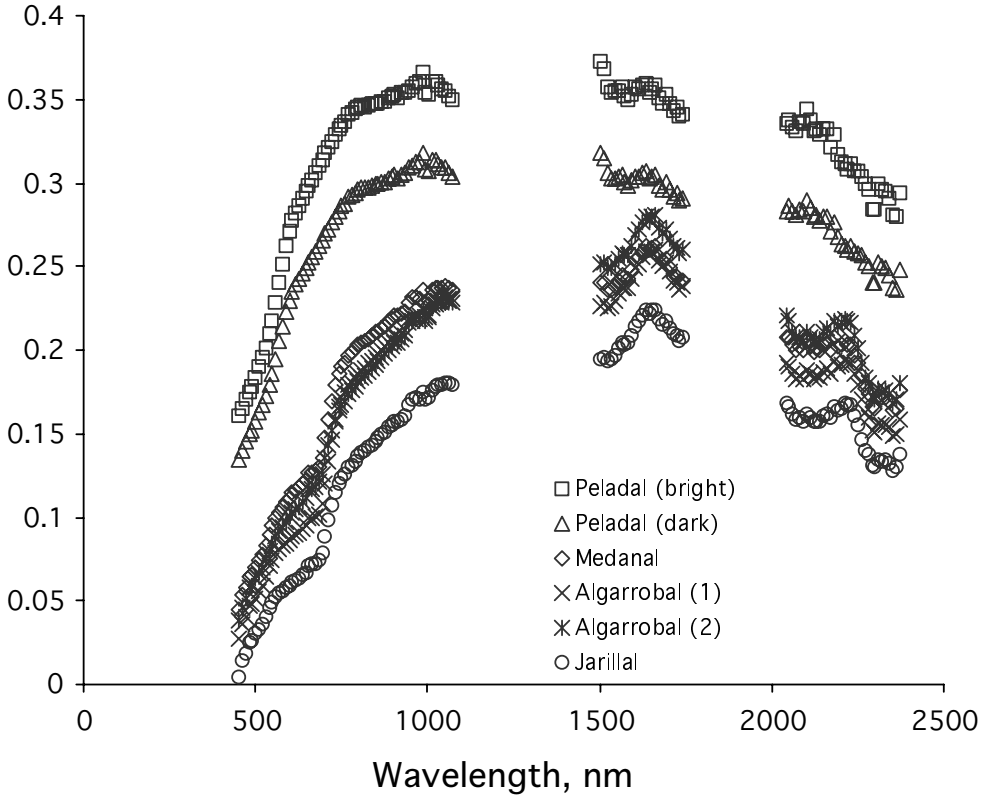

Figure 2. Averaged AV IRIS spectra of the main vegetation communities within and outside the Ñacuñán Biosphere Reserve.

An eigenanalysis of the AVIRIS hyperspectral data revealed a data dimensionality of 4 with 99.86% of the variance accounted for. The first 4 eigenvectors reveal the important spectral structure and signature curve shapes of the AVIRIS image (Fig. 3). The first eigenvector is equivalent to the mean spectral signature for the entire image and provides a brightness measure. The second eigenvector resembles green vegetation spectra. The 3rd and 4th eigenvectors resemble the non-photosynthetically active vegetation (NPV) spectral absorption features in the SWIR with unique absorption features relevant to the separation of NPV from soil and green vegetation (2080, 2210, and 2270 nm). The 4th eigenvector also show increasing secondary variations related to instrument noise but was retained for the information it contained in the SWIR.

Spectral mixture analysis was conducted by supplying 'pure' reference endmembers of known biophysical properties to transform and rotate the abstract PCA solution into a set of physically useful, fractional component images. The resulting fractional component images show very little difference in green vegetation (GV) between the inside and outside portions of the Ñacuñán reserve and there was no clear, discernable pattern of GV fractional values among the algarrobal, jarillal, and medanal communities inside the reserve (Fig. 4). The green vegetation fraction was lowest in the severely degraded peladal and moderately degraded medanal areas in the northern portion of the image. Green vegetation fractional amounts were also most variable in the peladal areas exhibiting minimal values in the severely degraded areas with adjacent high values due to clusters of cottonwood trees and mesquite growing at the edges of the denuded playas. These playas are used to harvest and store water, which sustain the cottonwood trees.

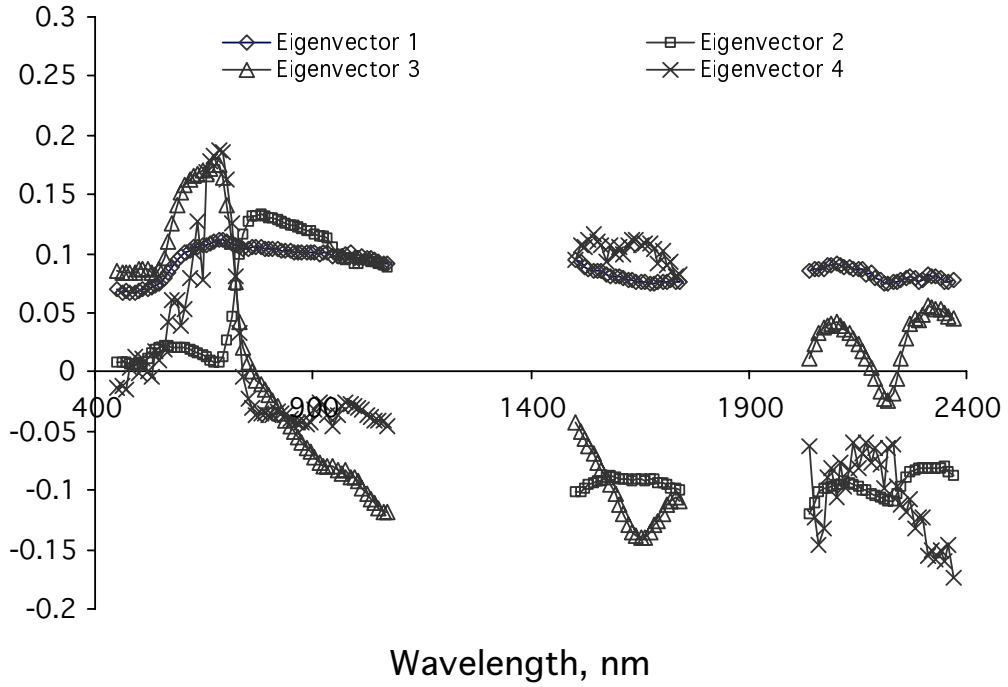

Figure 3. The first 4 primary eigenvectors derived from a principal components analysis of the AVIRIS image acquired over the Ñacuñán Biosphere Reserve.

The NPV signal was generally lower in the degraded northern part of the image consisting of medanal communities and was extremely low over the peladal areas (Fig. 4). As with the GV fraction, there were no discernable patterns of NPV among the vegetation formations within the reserve as well as in the immediate adjacent portions outside the reserve. There were larger differences in the soil fraction with darker soil values inside the reserve (Fig. 4). The soil fractional values were lowest in the jarillal communities (creosote bush) and highest in the degraded peladal communities outside and north of the reserve. The medanal site was of intermediate brightness and the algarrobal communities were slightly lower. The soil fraction for the algarrobal communities also appeared slightly darker inside the reserve compared with outside (Fig. 4). Fractional shade amounts also exhibited strong variability in the degraded peladal areas as a result of the dense trees casting shadows, surrounded by bare playas nearly devoid of vegetation canopy shade. Some of the clay playas, however, were extremely dry and cracked with crevices 20 – 30 cm wide and 10 – 20 cm deep, creating significant amounts of shade.

A scatterplot of the green vegetation fraction (GV) plotted against the NPV vegetation fraction for the range of sites, shows a general positive relationship in which increasing greenness is associated with higher values of NPV (Fig. 5). Both GV and NPV increase as the amount of vegetation increases, from the severely degraded peladal sites to the moderately degraded medanal (sand-dune) sites, and finally the healthy jarillal (creosote bush) and algarrobal (mesquite) communities. This formed a primary axis of total vegetation cover (GV + NPV) that enabled the separation of the various land degradation classes. A second axis of variation can also be seen whereby, within a given vegetation community, there is an inverse relationship between NPV and GV. This basically depicts the vegetation cover as either foliated (green leaves) or defoliated exposing the woody, NPV signal. For a given level of total plant cover, the proportions of GV and NPV will vary inversely, depending on environmental variables (soil moisture, meteorology) and phenology (dry season to wet season).

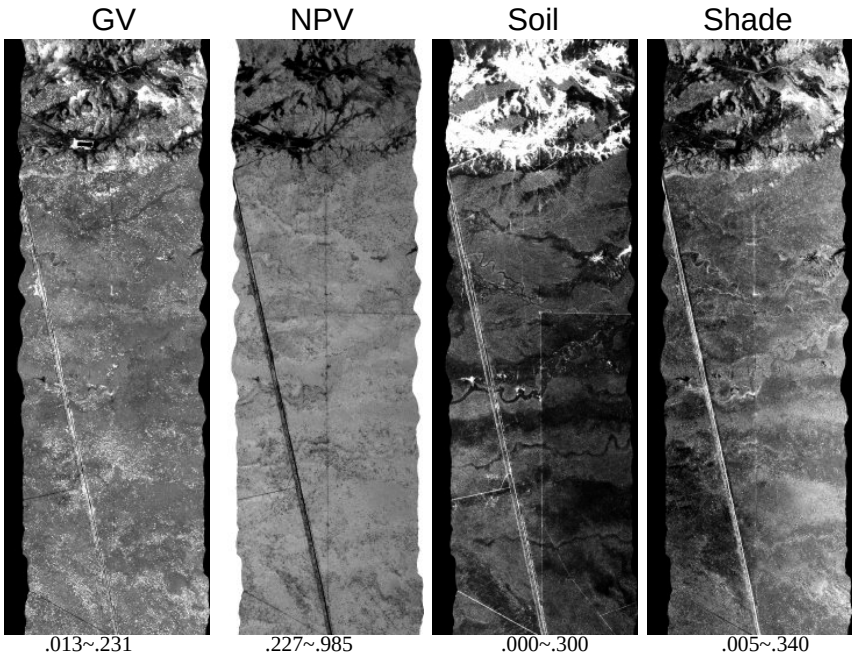

Figure 4. Fractional component images of the AVIRIS image data set over the Ñacuñán Biosphere Reserve, (a) GV, (b) NPV, (c) Soil, and (d) Shade images.

The two algarrobal sites represent sparse and dense 'green' vegetation, respectively. Note that the GV axis does not differentiate between the algarrobal and jarillal communities. The medanal site decreased in both GV and NPV, while the peladal areas were discriminable through either the GV or NPV fraction. Figure 5 depicts quite well the need for multiple landscape parameters for characterization and monitoring of land degradation. Neither greenness (GV) nor NPV components alone can discriminate the various vegetation communities and stages of land degradation due to the large overlap in vegetation properties. With these ambiguous signals, it would take much longer to reliably assess if land degradation is actually occurring. However, when GV and NPV are combined, one can note distinct clusters among the degradation classes and the trend of decreasing PV and NPV in shifting towards the origin with increasing degradation. A shift towards the origin indicates less total vegetation cover, which may be used as one reliable measure of land degradation.

The discrimination of the land degradation classes can also be observed in a plot of GV against the soil brightness signal (Fig. 6). There is an overall inverse relationship whereby as the vegetation fraction decreases as the soil component increases. However, the soil component not only increases in response to the greater proportion of exposed soil but also due to the 'brighter' soils found in the degraded areas (lower organic matter). This caused a shift toward higher soil values for a given amount of vegetation cover over the severely degraded peladal areas (Fig. 6). The soil component may thus be useful as a third landscape parameter for land degradation studies. As an example, the GV values of the medanal community were similar to those of the algarrobal community but were separable through the 'brighter' soil signal found in the degraded medanal site. Thus, the addition of the soil component information provided a means for further discrimination and landscape degradation analysis.

Similarly, Fig. 7 shows the much higher content of variance and information present in the fractional images of NPV, soil, and shade compared with green vegetation (GV) for the highly degraded areas north of the Reserve. Fence line boundaries with differing grazing patterns and management schemes are readily seen in the NPV, soil, and shade images but are nearly absent in the green vegetation fraction image.

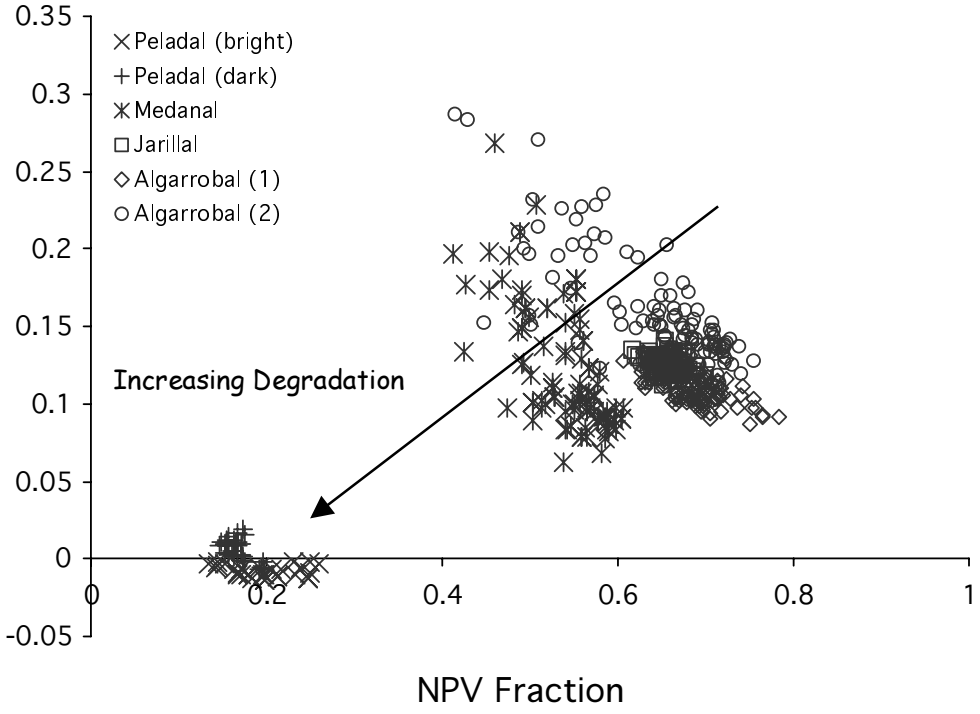

Figure 5. The green vegetation fractional component (GV) plotted against the NPV component for the major vegetation communities inside and outside the Ñacuñán Biosphere Reserve.

4. CONCLUSIONS AND DISCUSSION

The results of this study showed that simple 'greenness' measures, such spectral vegetation indices and GV fraction components, were not well adapted to the assessment of land degradation and desertification at the Ñacuñán Biosphere Reserve in Argentina. Land degradation in semiarid regions result in simultaneous changes in soil and vegetation optical properties involving the amount and composition/ structure of vegetation, the proportion of green (GV) and non-green (NPV), and the soil background. Spectral vegetation indices are limited in their ability to characterize such complex environments and may lead to ambiguous conclusions concerning land degradation. Greenness by itself will decrease with land degradation but will also shift greatly in response to seasonal variations as well as plant community composition changes with different proportions of GV and NPV (e.g., shifts from herbaceous to woody vegetation or shifts from perennial to annual vegetation).

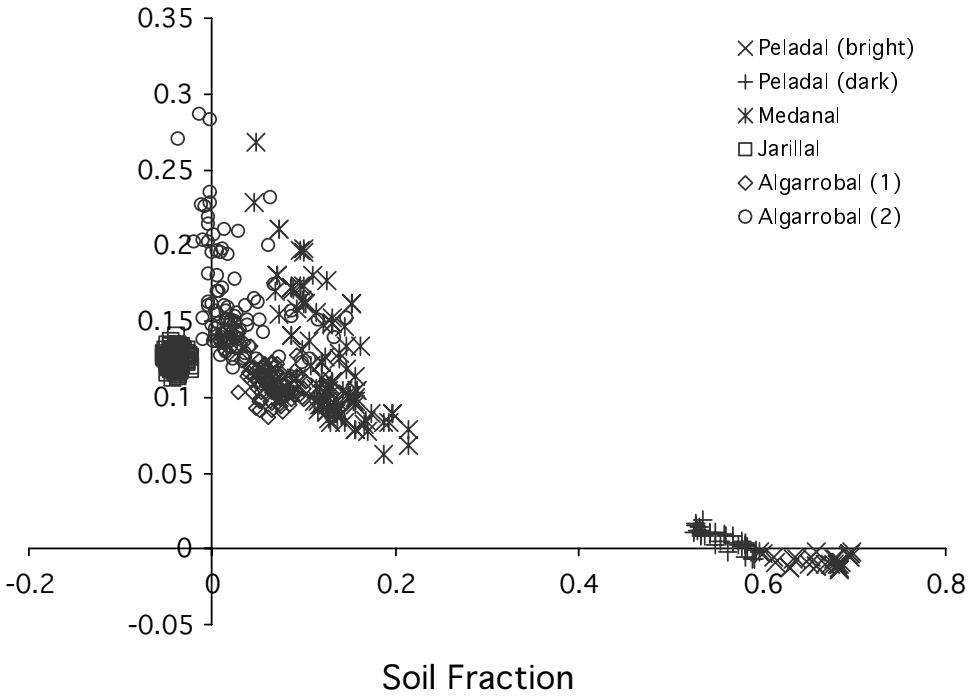

Figure 6. The green vegetation fractional component (GV) plotted against the soil component for the major vegetation communities inside and outside the Ñacuñán Biosphere Reserve.

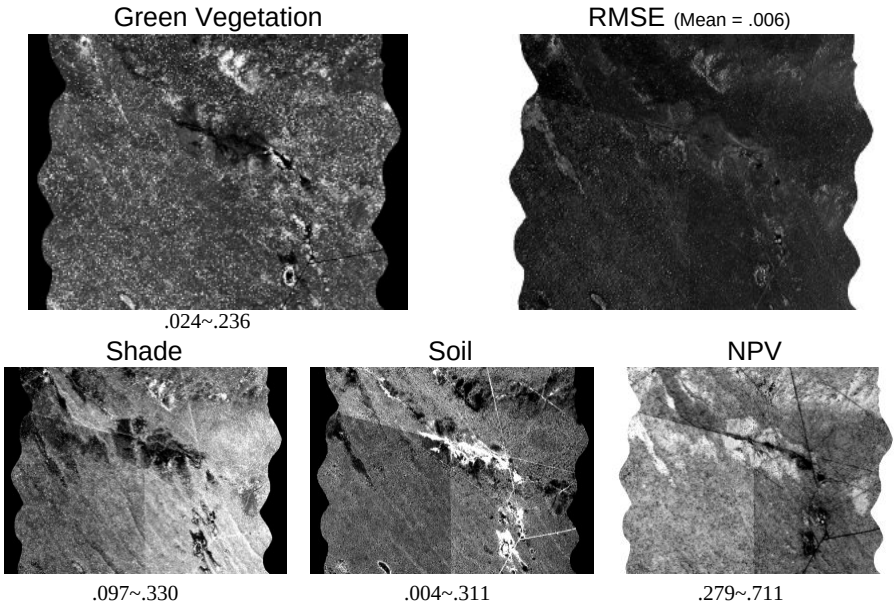

Figure 7. Fractional component images of the AVIRIS image data set in the degraded areas north of the Ñacuñán Biosphere Reserve, (a) GV, (b) RMSE, (c) Shade, (d) Soil, and (e) NPV images.

We found that land degradation was significantly improved with the inclusion of fractional NPV component information derived from spectral mixture analysis. The combination of NPV with PV enabled a more efficient and accurate characterization of the landscape with respect to natural vegetation communities and various stages of degradation. Whereas the separate GV and NPV fractional components could not differentiate many of the land degradation classes, they were able to do so in combination. The GV and NPV fractions enabled the assessment of total vegetation cover and allowed one to decouple differences in green vegetation resulting from phenology and vegetation composition across the landscape.

The soil fraction component also added useful information for better interpretations of land degradation. The soil background component is especially relevant for the monitoring of land degradation since the soil signal is generally dominant, highly variable, and vulnerable to large changes in areas undergoing degradation. Soil changes associated with land degradation are due to surface erosion, subsoil exposure, loss of soil carbon and moisture, and soil spatial heterogeneity. Land degradation invariably results in a stronger soil signal component to measured spectra and the spatial and temporal variations associated with the soil background must be decoupled from variations associated with vegetation in order to better interpret land degradation.

The extracted soil component from the mixture analysis was determined by two factors that created a certain degree of ambiguity to the interpretation of the mixture model results. The strength of the soil signal varied with the fractional amount of soil exposed as well as the inherent brightness of the soil. Thus, increases in the soil signal were the result of less vegetation cover (GV and NPV) as well as higher soil reflectances associated with degradation (crusting, less moisture, less organic carbon, erosion). There are more advanced methods of spectral mixture analysis that aim to extract the soil reflectance signal independent of exposed soil fraction and vegetation influences (Okin et al., 2001; Palacios-Orueta et al., 1999).

The use of satellite observations to monitor land degradation processes has a promising future, particularly with the use of hyperspectral sensor systems that offer the potential of extracting soil and vegetation biogeophysical component information for a more complete land surface characterization. When these multiple optical parameters are combined with GIS, process models, and moderate resolution sensors for phenology determinations, then desertification can be more quantitatively evaluated and monitored and the different processes that contribute to desertification (erosion, salinization, denuding of soil, overgrazing, water resources) can be assessed. The Earth Orbiter 1 (EO-1), launched in November 2000 as part of NASA's New Millennium program, includes a hyperspectral imager, Hyperion. The Hyperion hyperspectral imager is a pushbroom sensor providing 220, 10 nm bands covering the spectrum from 400 to 2500 nm. A space-based hyperspectral sensor with consistent and repeat observation capabilities will greatly improve land degradation monitoring and provide early warning detection capabilities.

5. ACKNOWLEDGMENTS

Greg Asner and Kathy Heidebrecht also provided help in site locations and provided calibration spectra and photos to help with our analyses. This work was supported by the NASA EO-1 grant NCC5-478 (A.R. Huete).

6. REFERENCES

Aguiar, M.R., Paruelo, J.M., Golluscio, R.A., León, R.J.C., Burkart, S.E., and Pujol, G., 1988, "The heterogeneity of the vegetation in arid and semiarid Patagonia: an analysis using AVHRR/NOAA satellite imagery," *Annali di Botanica,* 46:103-114.

Archer, S., Schimel, D., and Holland, E., 1995, "Mechanisms of shrubland expansion: land use, climate, or CO_2?," *Climatic Change,* 29:91-99.

Asner, G.P., and Green, R.O., 2002, "Imaging spectroscopy measures desertification in United States and Argentina," *EOS Trans.* 82 (49):601.

Asner, G.P. and Lobell, D.B., 2000, "A biogeophysical approach for automated SWIR unmixing of soils and vegetation," *Remote Sensing of Environment,* 74:99-112.

Gao, B.C. and Goetz, A.F.H., 1994, "Extraction of dry leaf spectral features from reflectance spectra of green vegetation," *Remote Sensing of Environment,* 47:369-374.

Ojeda, R.A., Campos, C.M., Gonnet, J.M., Borghi, C.E., and Roig, V.G., 1998, "The MaB reserve of Ñacuñan, Argentina: its role in understanding the Monte Desert biome," *J. Arid Environ.,* 39:299-313.

Okin, G.S., Roberts, D., Murray, B., and Okin, W.J., 2001, "Practical limits on hyperspectral vegetation discrimination in arid and semiarid environments," *Remote Sensing of Environment,* 77:212-225.

Palacios-Orueta, A., Pinzón, Ustin, S.L., and Roberts, D.A., 1999, "Remote sensing of soils in the Santa Monica Mountains: II. Hierarchical foreground and background analysis," *Remote Sensing of Environment,* 68:138-151.

Pickup, G., and Nelson, J., 1984, "Use of Landsat radiance parameters to distinguish soil erosion, stability and deposition in arid central Australia," *Remote Sens. Environ.*, 16:195-204.

Schlesinger, W.H., Reynolds, J.F., Cunningham, G.L., et al., 1990, "Biological feedback in global desertification," *Science*, 247:1043-1048.

Smith, M.O., Ustin, S.L., Adams, J.B., and Gillespie, A.R., 1990, "Vegetation in deserts: 1. A regional measure of abundance from multispectral images," *Remote Sens. Environ.* 31:1-26.

Tucker, C.J. and Nicholson, S.E., 1999, "Variations in the size of the Sahara Desert from 1980 to 1997," *Ambio*, 28:587-591.